Available online at BCREC website: https://bcrec.id

Bulletin of Chemical Reaction Engineering & Catalysis, 14 (3) 2019, 542-550

Research Article

Synthesis of Spherical Nanostructured γ-Al_2O_3 Particles using Cetyltrimethylammonium Bromide (CTAB) Reverse Micelle Templating

Didi P. Benu[1,3], Veinardi Suendo*[,1,2], Rino R. Mukti[1,2], Erna Febriyanti[1], Fry V. Steky[1], Damar R. Adhika[2], Viny V. Tanuwijaya[2], Ashari B. Nugraha[2]

[1]Division of Inorganic and Physical Chemistry, Faculty of Mathematics and Natural Sciences, Institut Teknologi Bandung, Jl. Ganesha No. 10, Bandung 40132, Indonesia
[2]Research Center for Nanosciences and Nanotechnology, Institut Teknologi Bandung, Jl. Ganesha No. 10, Bandung 40132, Indonesia
[3]Department of Chemistry, Universitas Timor, Jl. Eltari, Kefamenanu 85613, Indonesia

Received: 7th December 2018; Revised: 8th May 2019; Accepted: 20th May 2019; Available online: 30th September 2019; Published regularly: December 2019

Abstract

We demonstrated the synthesis of spherical nanostructured γ-Al_2O_3 using reverse micelle templating to enhance the surface area and reactant accessibility. Three different surfactants were used in this study: benzalkonium chloride (BZK), sodium dodecyl sulfate (SDS) and cetyltrimethylammonium bromide (CTAB). We obtained spherical nanostructured particles only using CTAB that form a reverse micelle emulsion. The particles have wide size distribution with an average size of 2.54 μm. The spherical particles consist of nanoplate crystallites with size 20-40 nm randomly arranged forming intercrystallite spaces. The crystalline phase of as-synthesized and calcined particles was boehmite and γ-Al_2O_3, respectively as determined by XRD analysis. Here, the preserved particle morphology during boehmite to γ-Al_2O_3 transformation opens a facile route to synthesize γ-Al_2O_3 particles with complex morphology. The specific surface area of synthesized particles is 201 m^2/g, which is around five times higher than the conventional γ-Al_2O_3 (Aldrich 544833). Spherical nanostructured γ-Al_2O_3 provides wide potential applications in catalysis due to its high density closed packed structure, large surface area, and high accessibility.

Keywords: Boehmite; CTAB; reverse micelle; spherical nanostructured particle; γ-Al_2O_3

How to Cite: Benu, D.P., Suendo, V., Mukti, R.R., Febriyanti, E., Steky, F.V., Adhika, D.R., Tanuwijaya, V.V., Nugraha, A.B. (2019). Synthesis of Spherical Nanostructured γ-Al_2O_3 Particles using Cetyltrimethylammonium Bromide (CTAB) Reverse Micelle Templating. *Bulletin of Chemical Reaction Engineering & Catalysis*, 14(3): 542-550 (doi:10.9767/bcrec.14.3.3855.542-550)

Permalink/DOI: https://doi.org/10.9767/bcrec.14.3.3855.542-550

1. Introduction

Alumina has been frequently reported as an important material in the field of catalysis, especially its polymorph, gamma alumina (γ-Al_2O_3) [1-5]. This material is very important as a catalyst or catalyst support due to its stability at high temperature and abundant Lewis acid sites [6-9]. The commonly used material as catalyst support is the conventional mesoporous γ-Al_2O_3 with closed channel structure formed by the inter-crystalline space [10-13]. Thus, the accessibility of reactants to the catalyst active sites is very limited. To have high catalytic per-

* Corresponding Author.
E-mail : vsuendo@chem.itb.ac.id (V. Suendo)
Tel. : +62 815-7208-5125

formance, catalyst or catalyst support must have not only high surface area but also high accessibility. Catalyst or catalyst support with high accessibility provides active sites with high efficiency.

A wise strategy that must be considered to increase the accessibility of γ-Al_2O_3 is by modifying its morphology. Aggregated nanocrystallites morphology of the conventional mesoporous γ-Al_2O_3 might only provide pores with closed channel structure [12,13]. The common strategy to increase the surface area and pore volume in conventional mesoporous γ-Al_2O_3 is by reducing the crystallite size [14]. This strategy might be affect the number of active sites, but not its accessibility. To increase the accessibility, we can try to transform the pore structure from a closed channel to an open channel. Figure 1a and 1b illustrate the comparison of the transport of reactants inside pore between the closed channel and open channel structure. The presence of obstacle inside the closed channel pore will completely block the flow of reactants. In open channel pore, the flow of reactants still can reach the active sites through the open channel side. Structural transformation from closed channel to open channel can be interpreted by assembling the crystallites into a conformation with open channel access. In the case of γ-Al_2O_3, we can employ this strategy by growing spherical γ-Al_2O_3 microparticles consist of randomly aggregated nanorod/nanoplate crystallites (Figure 1c).

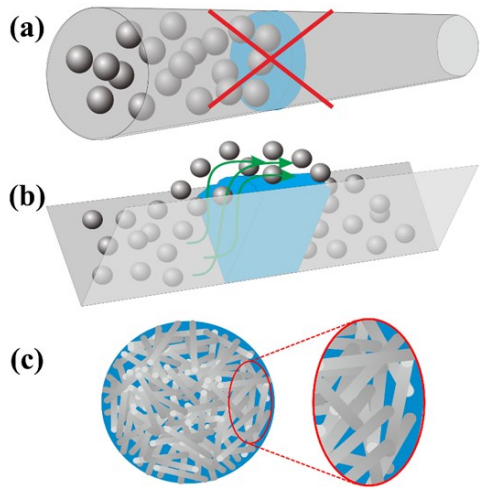

Figure 1. Illustration of reactant accessibility in catalyst support with (a) closed channel structure, (b) open channel structure. (c) Hypothetical representation of a spherical γ-Al_2O_3 microparticle consists of randomly aggregated nanorod crystallites.

Many research groups reported that γ-AlOOH (boehmite) can easily form γ-Al_2O_3 through calcination at a temperature of around 500 °C. This phase transformation has been studied theoretically [14] and experimentally [16-19]. The phase transformation occurred through the structural collapse of the boehmite framework after hydrogen transfer and internal water dehydration, followed by aluminum migration process [15]. The γ-Al_2O_3 with desired morphology only by controlling the morphology of boehmite can be synthesized. Thus, any desired morphology of γ-Al_2O_3 can be produced if we have the parent boehmite particles with the same desired morphology. This evidence has been reported by many research groups [20-22]. They successfully obtained nanostructured γ-Al_2O_3 with open channel structure from as-synthesized nanostructured boehmite with the same morphology. However, all reported methods above show a lack of controls on particle shape, separation and size. Here, synthesized γ-Al_2O_3 particles tend to form agglomerates.

One reported method that can control the shape, separation, and size of particles, is the reverse micelle templating method. Febriyanti and coworkers [23] successfully synthesized spherical nanostructured silica with bicontinuous concentric lamellar (*bcl*) morphology using CTAB reverse micelle as a template. In this study, we reported the synthesis of γ-Al_2O_3 using reverse micelle templating method to obtain nanostructured γ-Al_2O_3 with open channel structure.

2. Materials and Methods

2.1 Materials

$NaAlO_2$ and 1-butanol were purchased from Sigma Aldrich; toluene, urea, sodium dodecyl sulfate (SDS) and cetyltrimethylammonium bromide (CTAB) were purchased from Merck; benzalkonium chloride (BZK) solution Sanisol RC-A was purchased from Kao Chemicals. These reagents were used without any further purification. Tetraphenylporphyrin (TPP) solution was prepared by dissolving certain amount of TPP in toluene, while methylene blue (MB) solution was prepared by dissolving certain amount of MB in demineralized water.

2.2 Stable emulsion

To make a stable emulsion, firstly we made two mother solutions. The first solution is a polar phase (solution A) that contains $NaAlO_2$, BZK surfactant, urea, and water, while the sec-

ond solution is a nonpolar phase (solution B) that contains toluene and 1-butanol. The stable emulsion was made by adding solution A dropwise into solution B with vigorous stirring at 800 rpm for about 1 hour. The stable emulsion is a milky white mixture which does not breakdown without stirring. This process also applied to make any stable emulsions using both SDS and CTAB surfactants.

2.3 Emulsion test

The stable emulsion that previously obtained was tested using both the burn test and the dilution test. Burn test was carried out by immersing a toothpick into the emulsion and then burned the toothpick using a gas lighter. The toothpick will only be burned if the continuous phase of the emulsion is an oil phase or they formed a reverse micelle emulsion. The dilution test was performed to further confirm the formation of a reverse micelle emulsion. We performed the dilution test under a top illumination optical microscope Nikon Optiphot-100 POL with CF Plan objectives (10×) equipped with a Hayear CCD camera with two illumination types: a halogen lamp and a violet LED at 405 nm. Dilution test cell was prepared by dropping the emulsion onto the surface of a microscope slide and covering the emulsion droplet with a cover slip. The cover slip was fixed onto the microscope slide with a scotch tape keeping the cover slip from sliding. We then introduced a droplet of dye solution from the edge of cover slip. Here, we used two types of dye solution. Aqueous methylene blue (MB) solution represents the polar dye solution, while tetraphenylporphyrin (TPP) solution in toluene represents the nonpolar dye solution. Observations using MB solution were illuminated with a halogen lamp only, while observations using TPP solution were performed using both lamps. TPP solution gives a red fluorescence under a violet LED at 405 nm illumination. To have clear contrast observations between before and after applying MB or TPP solution into the emulsion system, the red color level of all obtained images was enhanced by shifting the green channel minimum value to 50 of 255 using ImageJ 1.52a, a public domain Java image processing program [24]. The emulsion type can be determined directly by observing how the dye solution penetrates into the emulsion under the cover slip. The steps of dilution test are illustrated schematically in Figure 2.

2.4 Synthesis of nanostructured γ-Al_2O_3

The γ-Al_2O_3 was synthesized by applying a solvothermal method. The stable emulsion was transferred into a Teflon-lined stainless-steel autoclave, sealed and heated in the oven at 160 ºC for 24 hours. The resulting product was filtered and rinsed with deionized water, ethanol,

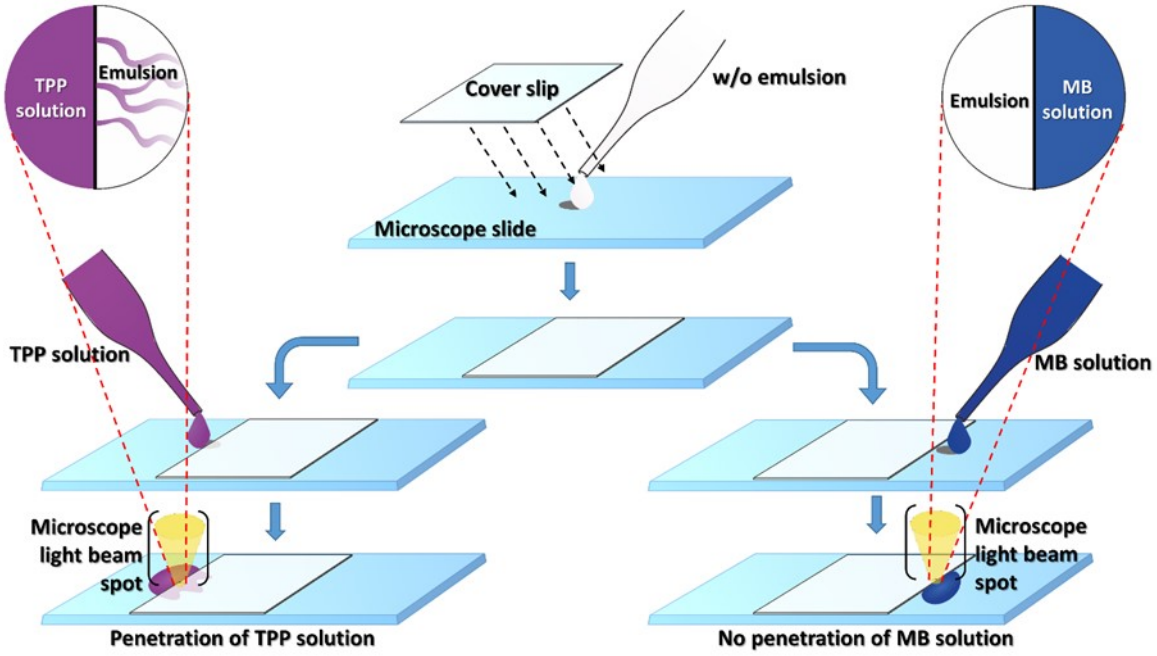

Figure 2. Schematic of dilution test procedure before observation of dye solution penetration under a top illumination optical microscope.

and acetone, respectively. The product was dried in the oven at 100 °C for 4 hours. Finally, the as-synthesized product was calcined at 550 °C for 4 hours in atmospheric pressure.

2.5 Material Characterizations

The morphology of resulting particles was observed using Scanning Electron Microscope (SEM) Hitachi SU3500 and High-Resolution Transmission Electron Microscope (HR-TEM) Hitachi H9500. From SEM images, we measured the diameter of 100 particles using ImageJ software and made a histogram plot to obtain particles size distribution. The TEM images were also analyzed using ImageJ software to obtain gray value profiles of particles. The XRD patterns were recorded on a Bruker Avance diffractometer with Cu Kα (λ = 1.54018 Å) radiation. N_2 physisorption measurement was carried out using a Quantachrome Nova 2000 surface area and pore size analyzer.

3. Results and Discussion

The essential requirement of material synthesis using reverse micelle templating method is to form a stable reverse micelle emulsion prior to any chemical reaction. The stable emulsion is an emulsion that will not break after the stirring is stopped. The surfactants used in this research were BZK, SDS, and CTAB. We only got the stable emulsion using SDS and CTAB surfactant. Burn tests show that SDS formed a normal micelle (o/w) emulsion, while CTAB formed a reverse micelle (w/o) emulsion. A surfactant can form either reverse micelle or normal micelle based on its HLB value. The hydrophilic-lipophilic balance (HLB) value of SDS surfactant is 40 in a range of normal micelle [25]. A reverse micelle can be formed when HLB in the range of 4-8. CTAB has HLB value of 7.375 that might form a reverse micelle emulsion based on HLB theory [25]. Figure 3 shows the evidence of CTAB forming a

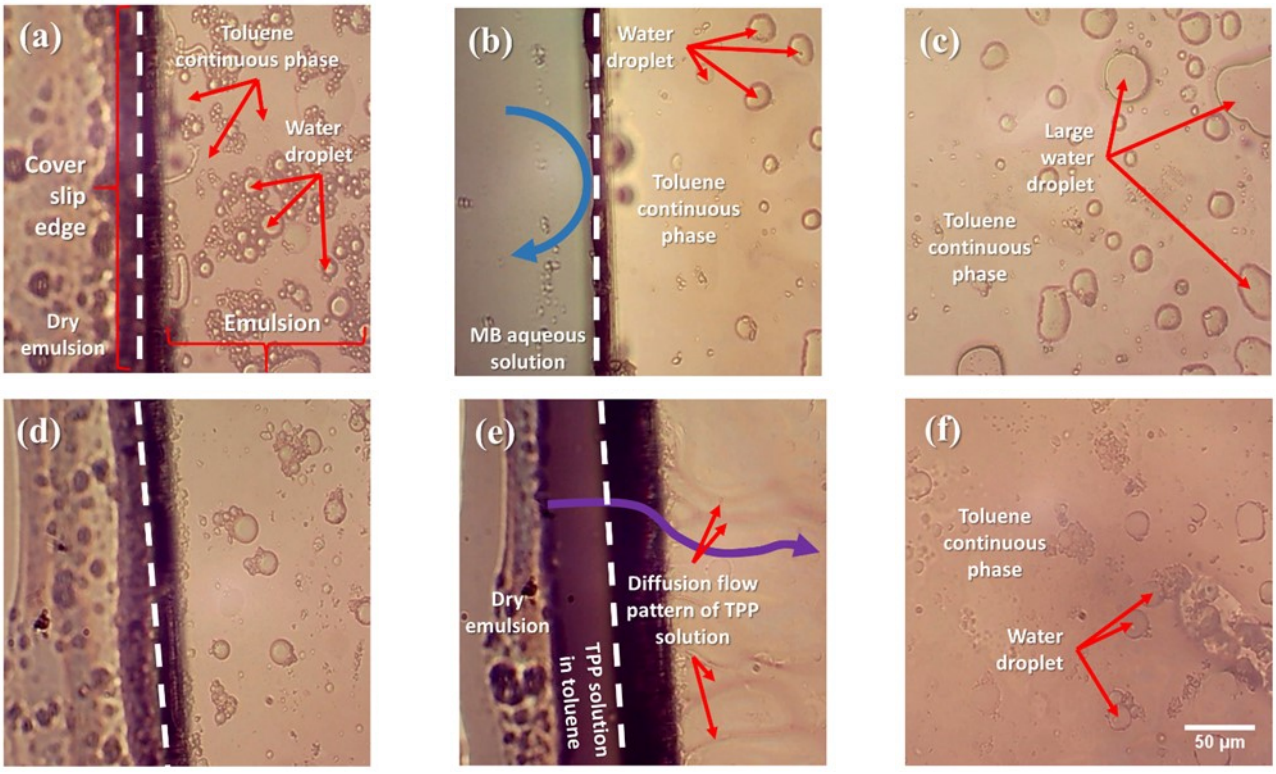

Figure 3. Microscope images of CTAB emulsions: (a) Before adding MB solution; (b) After adding MB solution: It shows a clear separation between emulsion and MB solution without penetration of MB solution into the emulsion; (c) Emulsion under the center part of cover slip shows no change in color; (d) Before adding TPP solution; (e) Shortly after adding TPP solution: It shows the penetration of TPP solution that diffuses into the emulsion; (d) Emulsion under the center part of cover slip shows change in color. The dashed white line represent the edge of cover slip that separates the dry emulsion (left) and the emulsion under cover slip (right).

reverse micelle emulsion based on the dilution test.

Figure 3a and 3d reveal the presence of droplets inside the continuous phase, indicating the emulsion is not a bicontinuous emulsion. To clarify the emulsion type, either it is a water-in-oil (w/o) or an oil-in-water (o/w) emulsion, we have to perform a dilution test. The dilution test is based on the interaction between probe dye solution (either diluted in a polar or a nonpolar solvent, i.e. water or toluene in our case, respectively) with the emulsion continuous phase. Figure 3b shows that the force generated when introducing the MB aqueous solution onto the edge of cover slip, pushes many droplets to the right direction without mixing the MB aqueous solution with the emulsion continuous phase. This indicates the emulsion continuous phase is toluene because it does not mix with water. A clear boundary between MB aqueous solution and emulsion phases is also observed in Figure 3b. This suggests that dry emulsion was dissolved by the presence of MB aqueous solution. In Figure 3c, we can see that the color of the emulsion continuous phase is not altered by the introduction of MB aqueous solution. This signifies that MB cannot dissolve in toluene as the emulsion continuous phase. The presence of large droplets due to penetration of water droplets that partly formed from the dissolved dry emulsion was also observed.

A totally different result was obtained when introducing the TPP solution onto the edge of the emulsion. The TPP solution diffuses easily into the emulsion continuous phase that observed as the diffusion flow patterns (see Figure 3e). These violetish flow patterns slowly changes color of the emulsion continuous phase. Figure 3f shows the violetish red color of emulsion continuous phase under the center part of cover slip due to the continuous diffu-

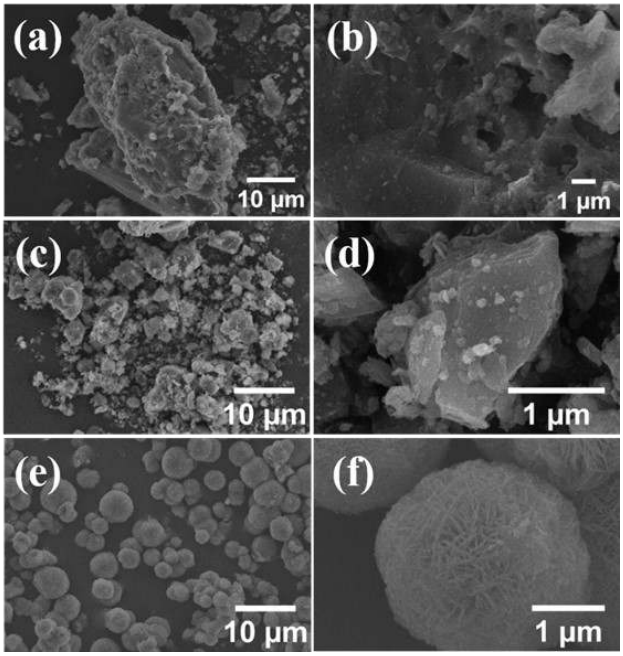

Figure 4. SEM images of synthesized particles using different surfactants; (a,b) BZK, (c,d) SDS, (e,f) CTAB. (b), (d) and (f) showing SEM images at high magnification.

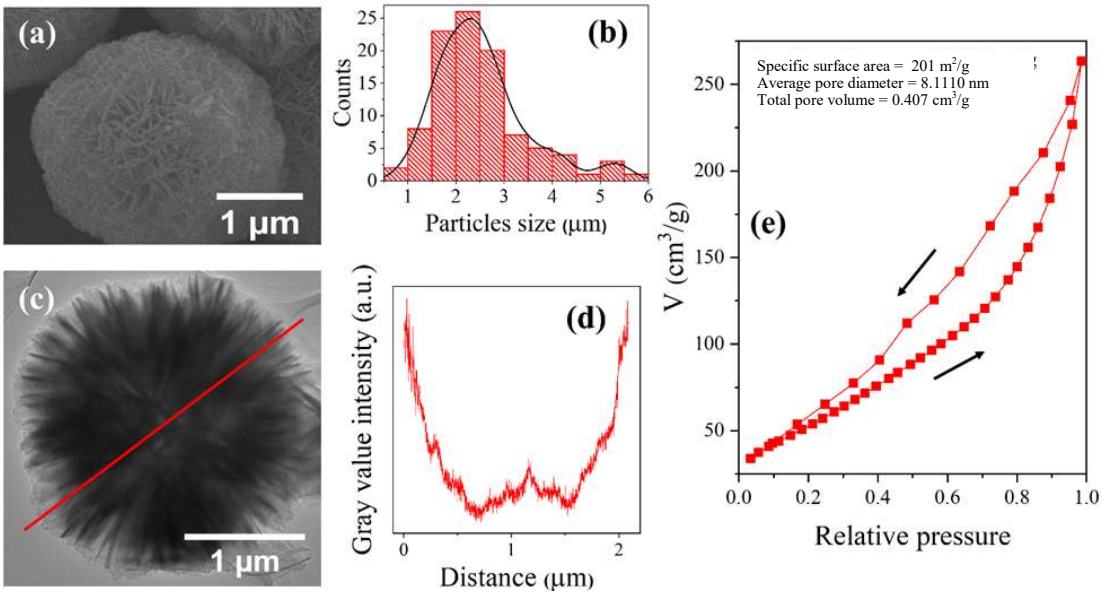

Figure 5. (a) SEM image; (b) particle size distribution; (c) N_2 Physisorption isotherm; (d) TEM image; (e) TEM profile of synthesized particle using CTAB surfactant forming a reverse micelle.

sion of TPP solution. The continuous phase of the emulsion is toluene and the droplets are water, or in the other word, the emulsion is a w/o emulsion or a reverse micelle system.

The morphology of synthesized particles using the three kinds of surfactant was shown in Figure 4. BZK surfactant did not provide any stable emulsion, thus the advantages of a reverse micelle (w/o) system are lost in this synthesis. This unstable emulsion may due to the formation of ion pairing between BZK cations and sodium aluminate anions (AlO_2^-). Ion pairing causes the micelles to lost their ability to repel each other, thus the emulsion becomes unstable and starts to coalesce. Based on the SEM images, synthesized particles using BZK surfactant give no regular shape and morphology. As shown in Figure 4a, the particles are aggregates without regularity. Figure 4b details the results with higher magnification, the surface of particles is dense without pores. The irregular shape and morphology are due to the formation of particles occurred in an unstable emulsion system. Thus, the growth of particles takes place in the water phase providing rapid and uncontrollable hydrolysis/condensation reaction resulting in particles with irregular morphology. Moreover, coalesced micelles cannot limit the growth of particles providing large particles with an irregular shape.

Because the failure of BZK surfactant to form a stable emulsion, then we used an anionic surfactant to prevent an ion pairing between surfactant and AlO_2^- ion. Using SDS surfactant, we get a stable emulsion. Although SDS surfactant formed a stable emulsion, the synthesized particles have no regular shape and morphology. Figure 4c shows the particles in the form of agglomerates without regularity. At high magnification in Figure 4d, particles have dense surfaces without pores or particular features. A normal micelle emulsion (o/w) consists of aqueous continuous phase that will not limit the growth of particles in the aqueous phase, such as hydrolysis/condensation reaction, but limit the reaction in the organic phase. Therefore, we cannot control the growth of boehmite particles in a normal micelle system.

It only gets a stable reverse micelle emulsion using CTAB surfactant. Figure 4e shows that CTAB reverse micelle results in spherical particles with wide size distribution. Figure 4f details the morphology of particle, showing aggregated nanoplates randomly arranged in a spherical cage forming a 3D open channel structure. Figure 5 shows the typical characteristics of synthesized particles using CTAB reverse micelle templating. In high magnification, it can be seen that the particles were composed of nanoplates with size 20-40 nm (Figure 5a). The particles have a size distribution in the range 0.5-6 μm and the average size of 2.54 μm (Figure 5b). This particular shape and morphology of particles were formed by nucleation and growth of crystallites in the water-pool of reverse micelle. The reverse micelle limits the growth of crystallites and directs their aggregation to form a spherical particle. The possible

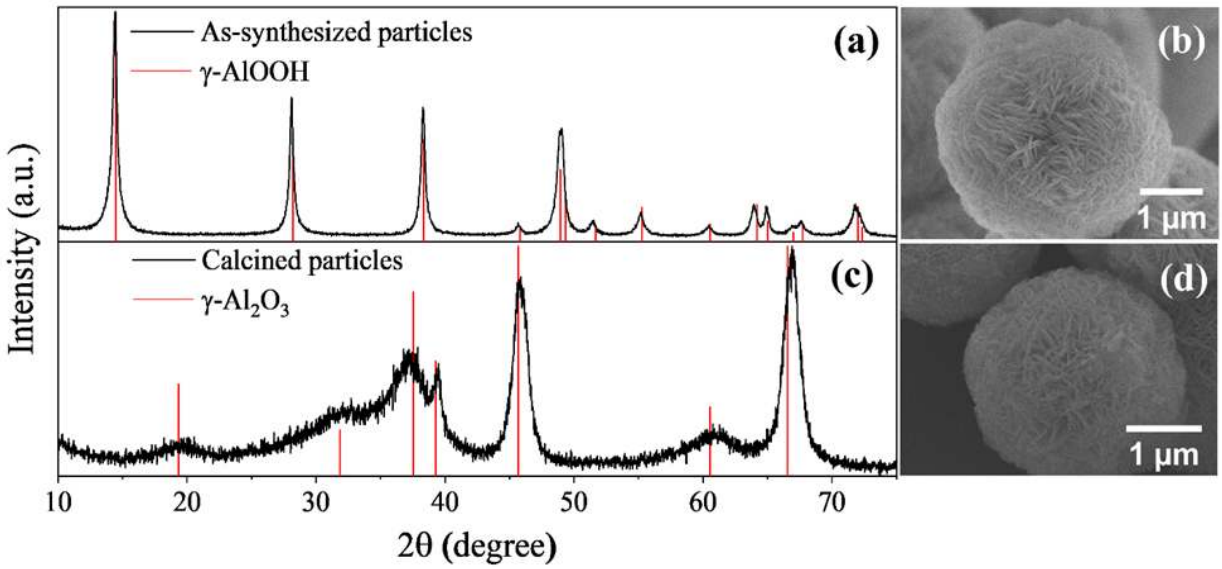

Figure 6. XRD patterns and SEM images of (a,b) as-synthesized and (c,d) calcined particles. The reference γ-AlOOH and γ-Al_2O are JCPDS card 021-1307 and JCPDS card 10-1245, respectively as published by Tang and coworkers [21].

formation of nanoplate is initiated by nucleation of seeds in the water-pool followed then by the growth of crystallites. The spherical shape of reverse micelle facilitates the self-assembly of the nanoplate crystallites to form a spherical particle consists of randomly arranged aggregated nanoplates. Spherical particles provide additional mechanical strength with respect to irregular shape particles due to their high density when they are arranged in a closed packed structure.

The internal morphology of synthesized particles using HR-TEM was also observed and analyzed the TEM profile using ImageJ software. Figure 5c reveals their internal morphology, where the nanoplates arranged randomly forming abundant open passages as depicted by bright areas. The bright areas represent the intercrystallite spaces between nanoplates. These open passages have interconnected each other deep into the center of the particle. This is confirmed by the presence of gray value intensity peaks in the center of the particle as shown in Figure 5d. These passages represent a 3D open channel structure.

Figure 5e shows N_2 Physisorption isotherm of synthesized particles using CTAB surfactant. The synthesized particle has a type IVa isotherm with H3 hysteresis loop. It indicates that the synthesized particles have a mesoporous characteristic with slit-shaped pores, when the pore width exceeds a certain critical width. The H3 hysteresis loop did not show any limiting adsorption at high relative pressure indicating non-rigid aggregates of plate-like particles [26]. This result is in a good agreement with morphological analysis using SEM and TEM, which the images depict spherical particles composed by nanoplates (see Figure 5a and 5c). The isotherm type also in a good agreement with the isotherm type of *bcl* silica with open channel structure [23], indicating the synthesized particle has open channel structure. From multi point BET analysis, the specific surface area of synthesized particles is 201 m^2/g. This specific surface area is much higher than the conventional γ-Al_2O_3 (Aldrich 544833), that is around 35-40 m^2/g [27-29]. From BJH analysis, we obtained the average pore diameter and total pore volume are 8.110 nm and 0.407 cm^3/g, respectively.

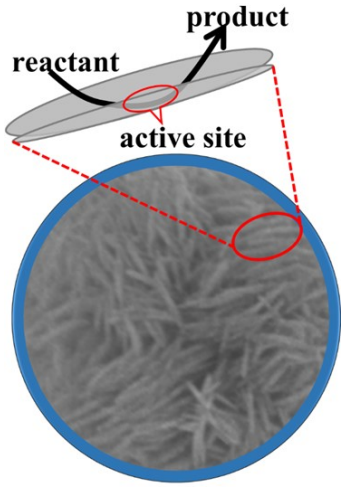

Figure 7. Illustration of reactant accessibility in γ-Al_2O_3 spherical nanostructured particles.

The structure of as-synthesized and calcined particles using XRD were also investigated. XRD patterns in Figure 6a and 6c, show that diffraction peaks of both as-synthesized and calcined particles are matched with their references the orthorhombic γ-AlOOH (JCPDS card 021-1307) and cubic γ-Al_2O_3 (JCPDS card 10-1245), respectively. No peaks from other phases are observed in both diffractograms indicating that the as-synthesized particles are boehmite and the calcined particles are γ-Al_2O_3, respectively. Any significant changes on particle morphology after calcination at 550 °C can not be seen (Figure 6b and 6d). It indicates that there is no massive structural deformation during boehmite to γ-Al_2O_3 transformation deteriorating particle morphology. Thus, nanostructured γ-Al_2O_3 can only be synthesized by controlling the shape and morphology of γ-AlOOH.

Open channel structures of γ-Al_2O_3 provide wide potential applications, such as catalyst or catalyst support due to its high accessibility. Figure 6 illustrates the reactants/products accessibility in γ-Al_2O_3 particles. The open channel structures facilitate the diffusion of reactants/products into/from the catalytic sites, respectively. This feature will break the diffusion limitation of the closed channel system and avoid the formation of cokes. The 3D arrangement of the open channels provides more accessible active sites than the conventional structure.

4. Conclusions

Spherical nanostructured γ-Al_2O_3 can only be obtained from a stable reverse micelle emulsion using CTAB. CTAB reverse micelle template successfully limits the growth of particles directing the formation of spherical γ-Al_2O_3 consists of randomly arranged nanoplates in a spherical cage. The specific surface area of synthesized particles is 201 m^2/g, which is around five times higher than the conventional γ-Al_2O_3

(Aldrich 544833). The aggregated nanoplates provide a 3D open channel structure with more accessible active sites. Spherical nanostructured γ-Al_2O_3 opens wide potential applications, notably in catalysis due to its high density closed packed structure, large surface area, and high accessibility.

Acknowledgments

This research was financially supported by *Penelitian Dasar Unggulan Perguruan Tinggi* (PDUPT) Research Grant No. 1/E/KPT/2018, Ministry of Research, Technology and Higher Education, Republic of Indonesia. D.P. Benu acknowledges *Lembaga Pengelola Dana Pendidikan* (LPDP) for scholarship support. E. Febriyanti acknowledges World Class University (WCU) Program, ITB for the postdoctoral program. F.V. Steky acknowledges Directorate General of Higher Education for *Bidik Misi* scholarship. Authors also acknowledge financial support from the Faculty of Mathematics and Natural Sciences, Institut Teknologi Bandung for participation in ICMNS 2018.

References

[1] Manton, M.R.S., Davidtz, J.C. (1997). Controlled pore sizes and active site spacings determining selectivity in amorphous silica-alumina catalysts. *Journal of Catalysis,* 60: 156-166.

[2] Schiffino, R.S., Merrill, R.P. (1993). A mechanistic study of the methanol dehydration reaction on γ-alumina catalyst. *J. Phys. Chem*., 97: 6425-6435.

[3] Trueba, M., Trasatti, S.P. (2005). γ-alumina as a support for catalysts: a review for fundamental aspects. *Eur. J. Inorg. Chem*., 2005(17): 3393–3403.

[4] Eliassi, A., Ranjbar, M. (2014). Application of novel gamma alumina nanostructure for preparation of dimethyl ether from methanol. *Int. J. Nanosci. Nanotechnol*., 10: 13-26.

[5] Ghosh, U., Kulkarni, K., Kulkarni, A.D., Chaudhari, P.L. (2015). Review-hydrocracking using different catalysts. *Chemical and Process Engineering Research*, 34: 51-55.

[6] McHale, J.M., Auroux, A., Perrotta, A.J., Navrotsky, A. (1997). Surface energies and thermodynamic phase stability in nanocrystalline aluminas. *Science*, 277: 788−791.

[7] Fionov, A.V. (2002). Lewis acid properties of alumina-based catalyst: study by paramagnetic complexes of probe molecules. *Surface Science*, 507-510: 74-81.

[8] Feng, R., Liu, S., Bai, P., Qiao, K., Wang, Y., Al-Megren, H., Rood, M.J., Yang, Z. (2014). Preparation and characterization of γ-Al_2O_3 with rich Brønsted acid Sites and its application in the fluid catalytic cracking process. *J. Phys. Chem. C*, 118: 6226−6234.

[9] Wu, Q., Zhang, F., Yang, J., Li, Q., Tu, B., Zhao, D. (2011): Synthesis of ordered mesoporous alumina with large pore sizes and hierarchical structure, *Microporous, and Mesoporous Materials*. 143: 406–412.

[10] Zhong, L., Zhang, Y., Zhang, Y. (2011). Cleaner synthesis of mesoporous alumina from sodium aluminate solution. *Green Chem*., 13: 2525-2530.

[11] Khazaei, A., Nazari, S., Karimi, G., Ghaderi, E., Moradian, K.M., Bagherpor, Z., Nazari, S. (2016). Synthesis and characterization of γ-alumina porous nanoparticle from sodium aluminate liquor with two different surfactants. *Int. J. Nanosci. Nantechnol,* 12: 207-214.

[12] Huang, B., Bartholomew, C.H., Woodfield, B.F. (2014). Facile synthesis of mesoporous c-alumina with tunable pore size: The effects of water to aluminum molar ratio in hydrolysis of aluminum alkoxides. *Microporous and Mesoporous Materials,* 183: 37–47.

[13] Wu, W., Wan, Z., Zhu, M., Zhang, D. (2016). A facile route to aqueous phase synthesis of mesoporous alumina with controllable structural properties. *Microporous and Mesoporous Materials*, 223: 203-212.

[14] Keshavarz, A.R., Rezaei, M., Yaripour, F. (2010). Nanocrystalline gamma-alumina: A highly active catalyst for dimethyl ether synthesis. *Powder Technology*, 199: 176–179.

[15] Krokidis, X., Raybaud, P., Gobichon, A., Rebours, B., Euzen, P., Toulhoat, H. (2001). Theoretical study of the dehydration process of boehmite to γ-alumina, *J. Phys. Chem. B*, 105: 5121-5130.

[16] Paglia, G., Buckley, C.E., Rohl, A.L., Hart, R.D., Winter, K., Studer, A.J., Hunter, B.A., Hanna, J.V. (2004). Boehmite derived γ-alumina system. 1. Structural evolution with temperature, with the identification and structural determination of a new transition phase, γ'-Alumina. *Chem. Mater*., 16: 220-236.

[17] Alphonse, P., Courty, M. (2005). Structure and thermal behavior of nanocrystalline boehmite. *Thermochimica Acta*, 425: 75–89.

[18] Boumaza, A., Djelloul, A., Guerrab, F. (2010). Specific signatures of α-alumina powders prepared by calcination of boehmite or gibbsite, *Powder Technology*, 201: 177–180.

[19] Alex, T.C. (2014). An insight into the changes in the thermal analysis curves of boehmite with mechanical activation, *J. Therm. Anal. Calorim.*, 117: 163–171.

[20] Li, G., Liu, Y., Liu, D., Liu, L., Liu, C. (2010). Synthesis of flower-like *boehmite* (AlOOH) via a simple solvothermal process without surfactant, *Materials Research Bulletin*, 45: 1487–1491.

[21] Tang, Z., Liang, J., Li, X., Li, J., Guo, H., Liu, Y., Liu, C. (2013). Synthesis of flower-like *boehmite* (γ-AlOOH) via a one-step ionic liquid-assisted hydrothermal route, *Journal of Solid-State Chemistry,* 202: 305–314.

[22] Wang, Z., Du, H., Gong, J., Yang, S., Ma, J., Xu, J. (2014). Facile synthesis of hierarchical flower-like γ-AlOOH films via hydrothermal route on quartz surface. *Colloids and Surfaces A: Physicochemical and Engineering Aspects,* 450: 76-82.

[23] Febriyanti, E., Suendo, V., Mukti, R.R., Prasetyo, A., Akbar, M.A., Triwahyono, S., Marsih, I.M., Ismunandar, I. (2016). Further insight into the definite morphology and formation mechanism of mesoporous silica KCC-1, *Langmuir,* 32: 5802-5811.

[24] Schneider, C.A., Rasband, W.S.,Eliceiri, K.W. (2012): NIH Image to ImageJ: 25 years of image analysis, *Nature methods*, 9(7): 671-675.

[25] Davies, J.T. (1957). A quantitative kinetic theory of emulsion type. I. Physical chemistry of the emulsifying agent, *Proceedings of 2nd International Congress Surface Activity,* London, 426-438.

[26] Thommes, M., Kaneko, K., Neimark, A.V., Olivier, J.P., Rodriguez-Reinoso, F., Rouquerol, J., Sing, K.S.W. (2015). Physisorption of gases, with special reference to the evaluation of surface area and pore size distribution (IUPAC Technical Report). *Pure and Applied Chemistry*, 87 (9–10): 1-19.

[27] Gould, T.D., Izar, A., Weimer, A.W., Falconer, J.L., Medlin, J.W. (2014). Stabilizing Ni catalysts by molecular layer deposition for harsh, dry reforming conditions. *ACS Catalysis,* 4 (8): 2714–2717.

[28] Gould, T.D., Lubers, A.M., Corpuz, A.R., Weimer, A.W., Falconer, J.L., Medlin, J.W. (2015). Controlling nanoscale properties of supported platinum catalysts through atomic layer deposition. *ACS Catalysis*, 5 (2): 1344–1352.

[29] M'rad, I., Jeljeli, M., Rihane, N., Hilber, P., Sakly, M., Amara, S. (2018). Aluminium oxide nanoparticles compromise spatial learning and memory performance in rats. *EXCLI Journal*, 17: 200-210.